

A comprehensive model for the coupled modelling of MnS inclusion and macrosegregation

Duanxing Cai^{1,2}, Jun Li¹, Hongbiao Dong¹, and Jianguo
Li²

¹University of Leicester, UK

²Shanghai Jiao Tong University, China

Outlines

1

Background

2

Model Description

3

Results

4

Summary

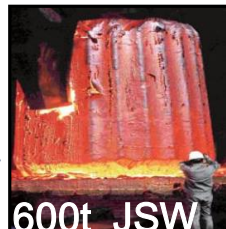
■ Motivation



Raw materials



smelting



600t JSW
Ingots making



Forging



Heat treatment



Product

1000MW nuclear
power plant

**Failure: 45% in casting+25%in forging+30% in heat
treatment**

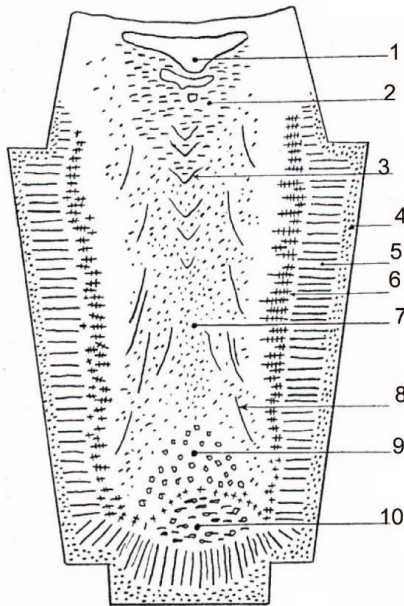
Forging: 3070 ton/suit

**Ingots casting is the first step, irreplaceable but also
bottleneck of large equipment manufacturing**

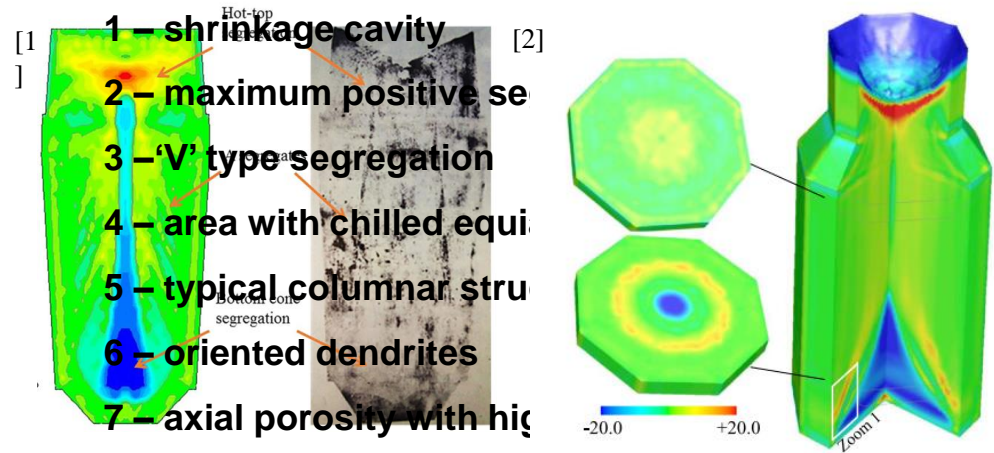
Ingots: **10,000** ton/suit

■ Motivation

➤ Typical defects & as-cast micro structure in large ingots



➤ Macrosegregation models



[1] D. Cai et al. Metal. Mater. Trans A 50 (2019) 1323-1332

[2] M. Wu et al. J. Mater. Res. 11, 41.

9 - cone of negative segregation

10 - inclusions

➤ The macrosegregation model of large ingot is well established without the efforts to predict the inclusion precipitate during solidification.

Outlines

1

Background

2

Model Description

3

Results

4

Summary

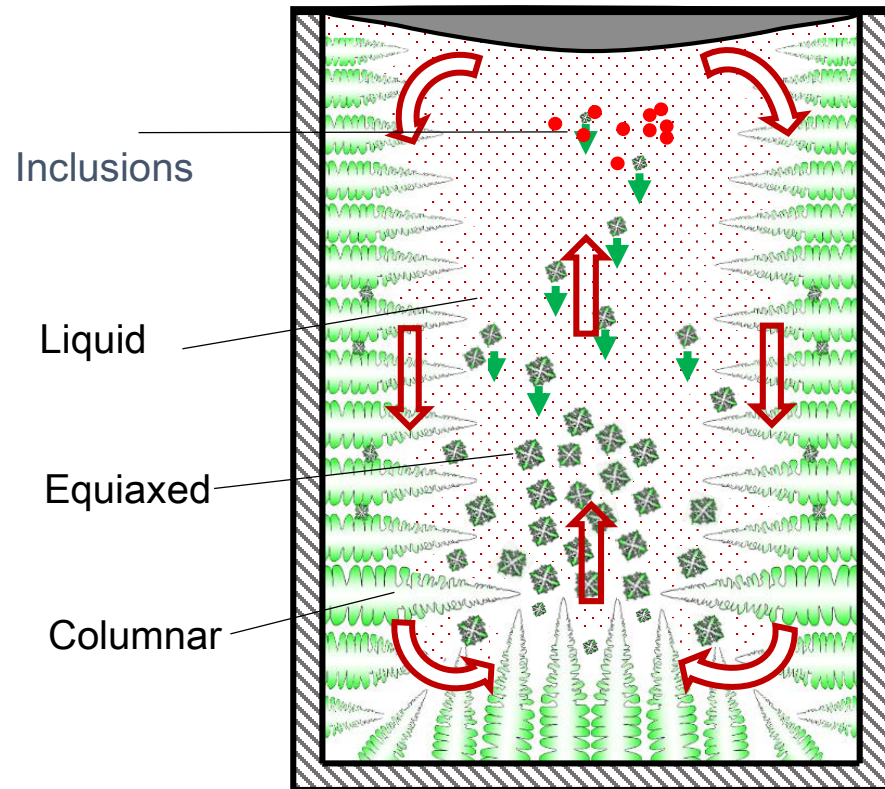
■ Phase Definition

➤ Phase definition:

- liquid
- equiaxed
- columnar
- inclusion

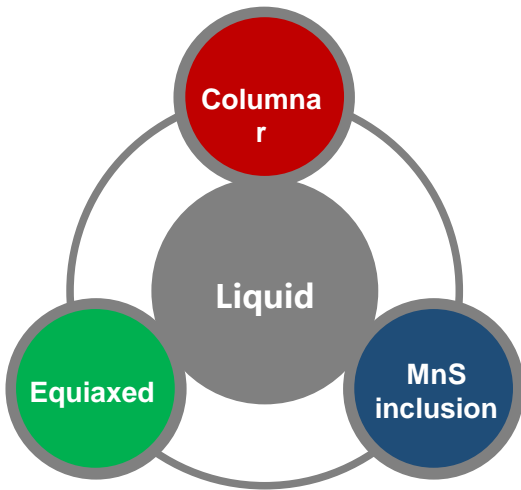
Average Volume Method

M. Wu and A. Ludwig, MMTA, 2006, 37A, 1613;
M. Wu and A. Ludwig, MMTA, 2008, 38A, 1465;
Ni and Beckermann, MMTB, 1991, 22, 349.



Ingot solidification schematic

■ Interaction between Each Phase



Nucleation of equiaxed grains:
$$N_e = \frac{d(\Delta T)}{dt} \cdot \frac{n_{\max}}{\sqrt{2\pi} \cdot \Delta T_\sigma} \cdot e^{-\frac{1}{2} \left(\frac{\Delta T - \Delta T_N^*}{\Delta T_\sigma} \right)^2}$$

Equiaxed growth rate:
$$v_{R_e} = \frac{dR_e}{dt} = \frac{D_\ell}{R_e (1 - R_e/R_{f,e})} \cdot \frac{c_\ell^* - c_\ell}{c_\ell^* - c_s^*}$$

Columnar growth rate:
$$v_{R_c} = \frac{dR_c}{dt} = \frac{D_\ell}{R_c} \cdot \frac{(c_\ell^* - c_\ell)}{(c_\ell^* - c_s^*)} \cdot \ln^{-1} \left(\frac{R_{f,c}}{R_c} \right)$$

Mass transfer rate from liquid to columnar:

$$M_{\ell c} = v_{R_c} \cdot n_c \cdot (\pi d_c \cdot l) \cdot \rho_\ell \cdot \Phi_{\text{impf}}$$

Mass transfer rate from liquid to equiaxed:

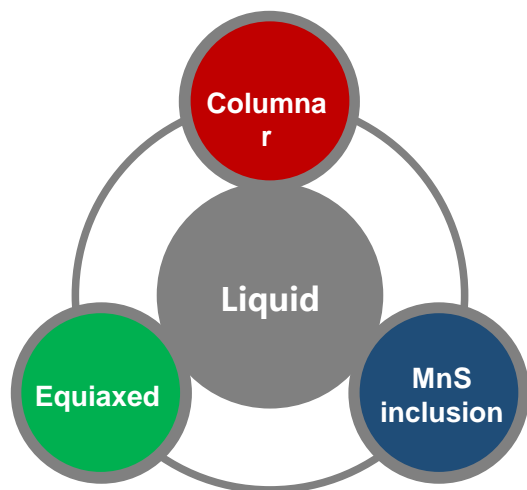
$$M_{\ell e} = v_{R_e} \cdot \left(n \cdot \pi d_e^2 \right) \rho_e \cdot \Phi_{\text{imp}}$$

Solute transfer rate from liquid to solid phase

$$C_{\ell s} = c^* \cdot M_{\ell s}$$

$$c^* = \begin{cases} k \cdot c_1^* & \text{(solidification)} \\ c_1 & \text{(remelting)} \end{cases}$$

Interaction between Each Phase



- M. Wu, et al, MMTA, 2006,37, 1613
 M. Wu, A. Ludwig, MMTA, 38A, 2007, pp. 1465
 A. Ludwig, M. MSEA,, 413-414, 2005, pp. 109
 J. Li, M. Wu, et. al, CMS, 2012, 79 : 830
 J, Li, M. Wu, et al, IJHMT, 2014, 72 : 668
 C. Wang, C. Beckermann, et al, MMTA, 1995, 26,111

Col./liquid drag. : Blake-Kozeny

$$K_{lc} = -\frac{f_l^2 \cdot \mu_l}{K} \quad K = 6 \times 10^{-4} \cdot \lambda_1^2 \cdot \frac{f_l^3}{(1-f_l)^2}$$

Equiaxed/liquid drag : Wang-Beckermann

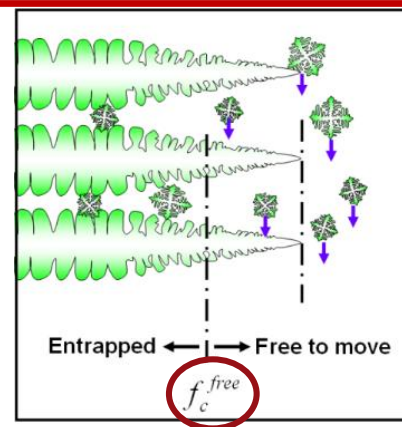
$$K_{le} = \frac{4\beta^2 \mu_l f_{l_total}^2}{d_e^2} \quad \beta = \frac{\beta_d}{\left[(1-\beta_e)^n + (\beta_d/\beta_e)^{2n} \right]^{1/2n}}$$

Col./equiaxed interaction :

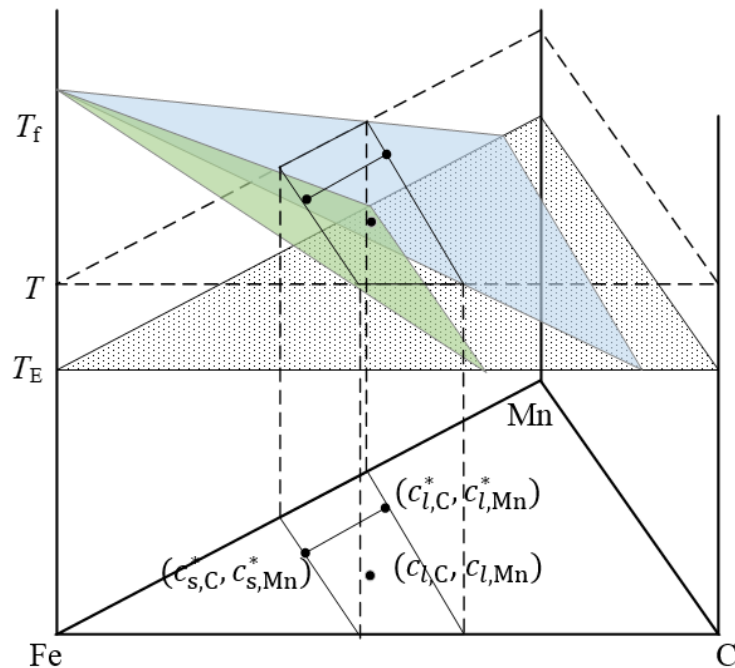
$f_c \geq f_c^{free}$: equiaxed entrapped

$f_c < f_c^{free}$: equiaxed free

Packing limit: $f_e + f_c \geq 0.637$



Basic Solution of Ternary Alloy



Fe-rich corner of an Fe-C-Mn linearized phase diagram

$$vR_C = \frac{dR_C}{dt} = \frac{D_{l,C}}{R_C} \cdot \frac{(c_{l,C}^* - c_{l,C})}{(c_{l,C}^* - c_{s,C}^*)} \cdot \ln^{-1} \left(\frac{R_{f,c}}{R_C} \right)$$

MnS. In almost every steel grade, causing serious damage to the properties of steel by acting as a potential starting point for

$$\frac{D_{l,C}}{R_C} \cdot \frac{(c_{l,C}^* - c_{l,C})}{(c_{l,C}^* - c_{s,C}^*)} = \frac{D_{l,Mn}}{R_{Mn}} \cdot \frac{(c_{l,Mn}^* - c_{l,Mn})}{(c_{l,Mn}^* - c_{s,Mn}^*)}$$

$T = T_{MnS} = T_{Mn} + \frac{v_{Mn}}{v_C} \ln \frac{c_{l,C}}{c_{l,Mn}} \frac{c_{s,Mn}^*}{c_{s,C}^*}$

crack formation or corrosion

Solution:

$c_{l,C}^*$	$c_{l,Mn}^*$
$c_{s,C}^*$	$c_{s,Mn}^*$

■ Modelling the MnS formation and growth

Thermodynamic criteria



$$K = c_{l,\text{Mn}} \cdot c_{l,\text{S}}$$

$$\log K_{\text{eq}} = -8750/T + 4.63$$

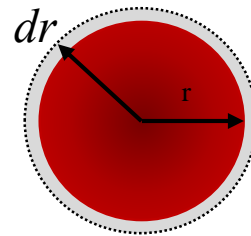
$c_{l,\text{S}}$ is calculated simply by Scheil law.

$$c_{l,\text{S}} = \frac{c_{0,\text{S}}}{(1-f_s)^{1-k_s}}$$

Nucleation rate of inclusion

$$\frac{\partial}{\partial t} n + \nabla \cdot (\vec{u} p n) = N_p = I_A \exp \frac{-\Delta G^*}{k_b T}$$

Growth rate



$$\text{A: } J_{\text{Mn}} = \left(\frac{\rho_p}{M_p} \right) \cdot \frac{dr}{dt}$$

$$\text{B: } J_{\text{Mn}} = \frac{D_{l,\text{Mn}}}{r} \cdot \frac{\rho_l}{100 \cdot M_{\text{Mn}}} \cdot (c_{l,\text{Mn}} - c_{p,\text{Mn}}^{\text{equilibrium}})$$

$$v_{\text{Rp}} = \frac{M_p \rho_l}{100 \cdot M_{\text{Mn}} \rho_p} D_{l,\text{Mn}} (c_{l,\text{Mn}} - c_{p,\text{Mn}}^{\text{equilibrium}})$$

Outlines

1

Background

2

Model description

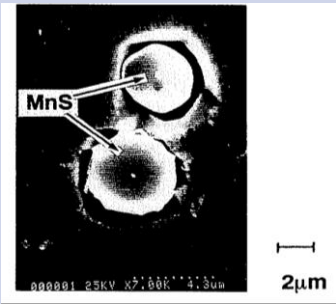
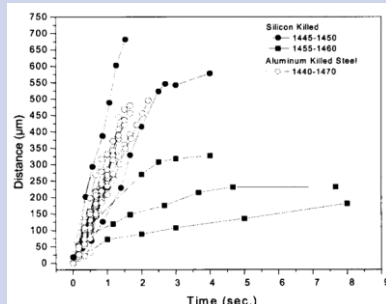
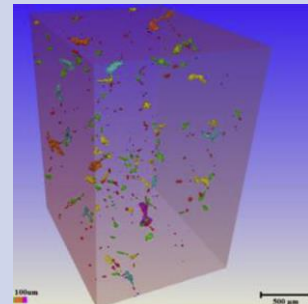
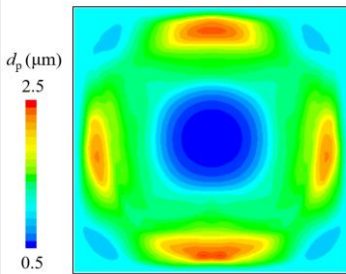
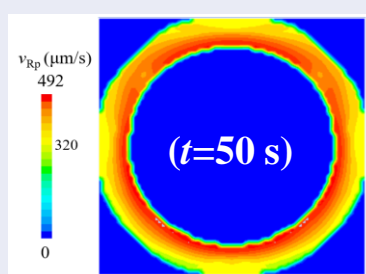
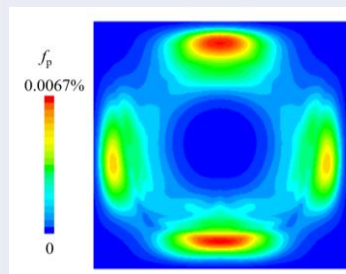
3

Results

4

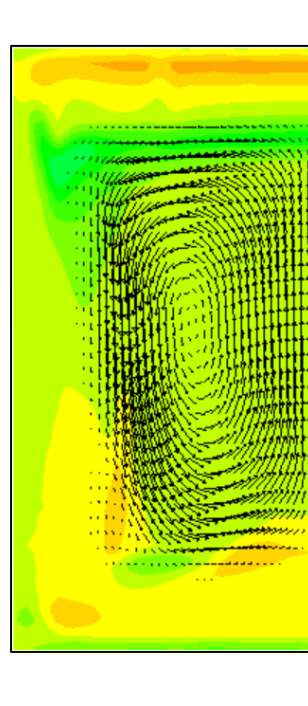
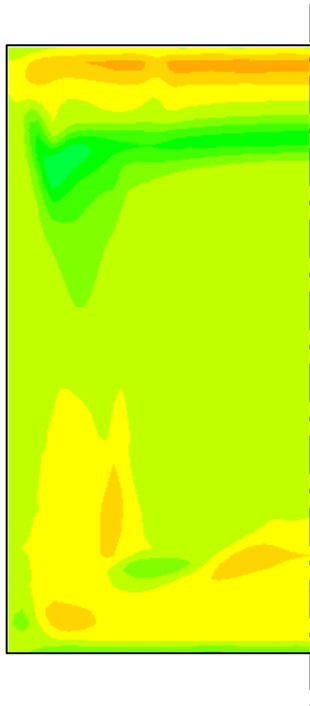
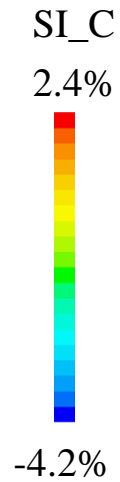
Summary

■ Experimental verification

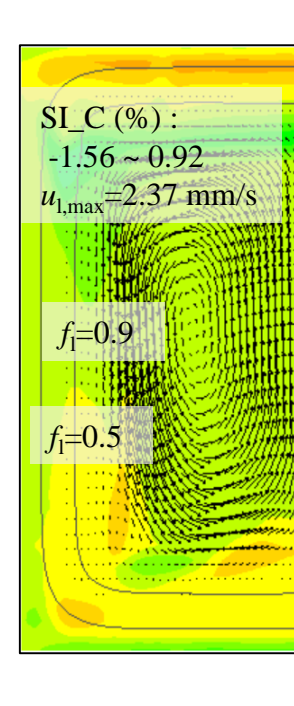
Comparison	Diameter (μm)	Growth velocity ($\mu\text{m/s}$)	Volume fraction
Experimental data	<p>W. M. (1996). <i>ISIJ inter.</i>, 36(8), 1014-1021.</p>  <p>Range: [0.5-6]</p>	<p>Valdez, M. E <i>Steel research inter.</i>, 75(4), 247-256.</p>  <p>Range: [60-500]</p>	<p>Cao, Y. F <i>Acta Mater.</i>, 107, 325-336.</p>  <p>Range: [0.087%-0.26%]</p>
Calculated results			

■ Evolution of Macrosegregation

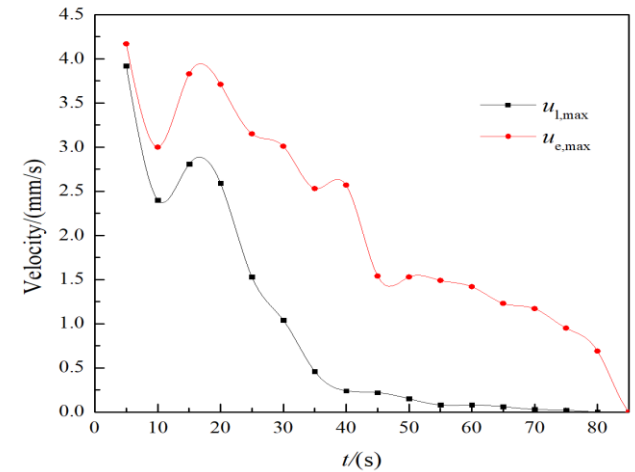
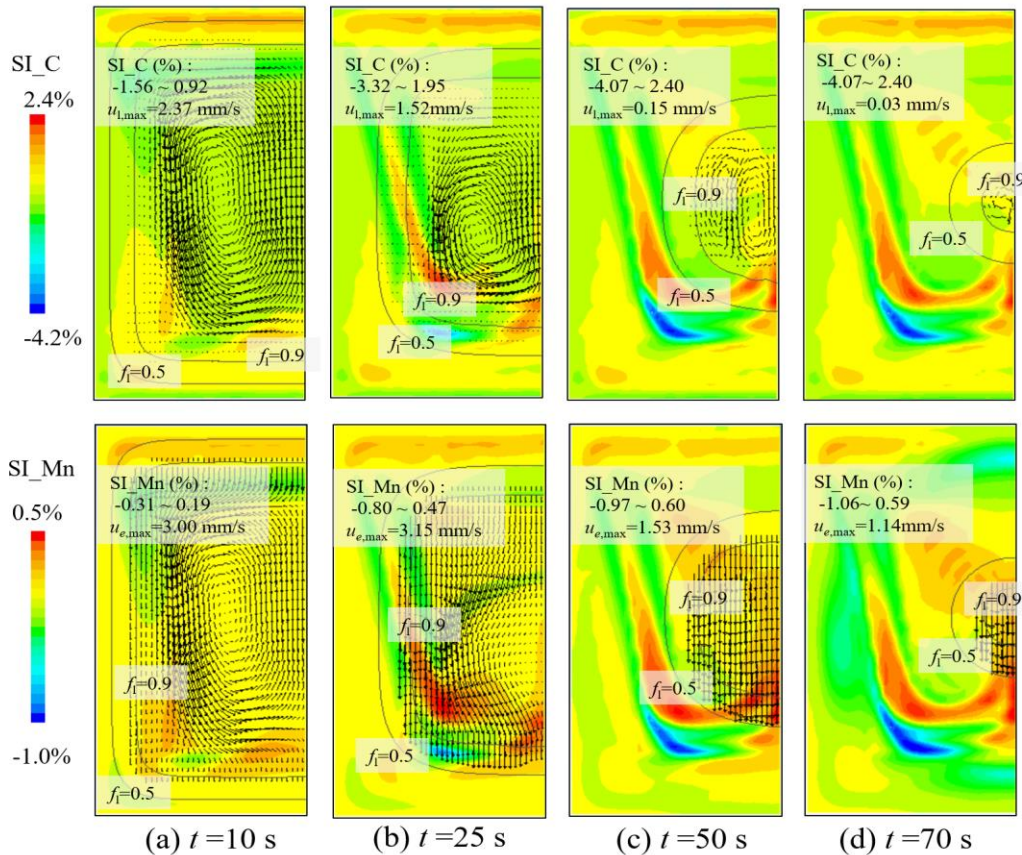
Segregation index (SI) = $(c_1 - c_0)/c_0$



$t = 10$ s

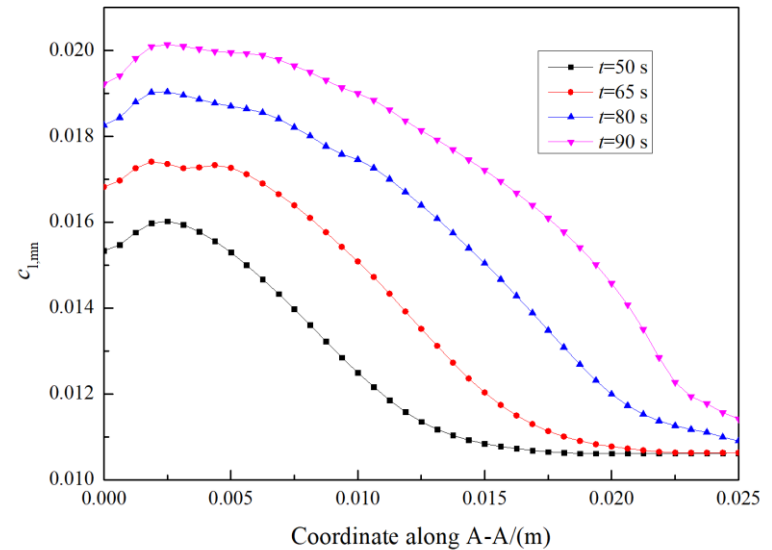
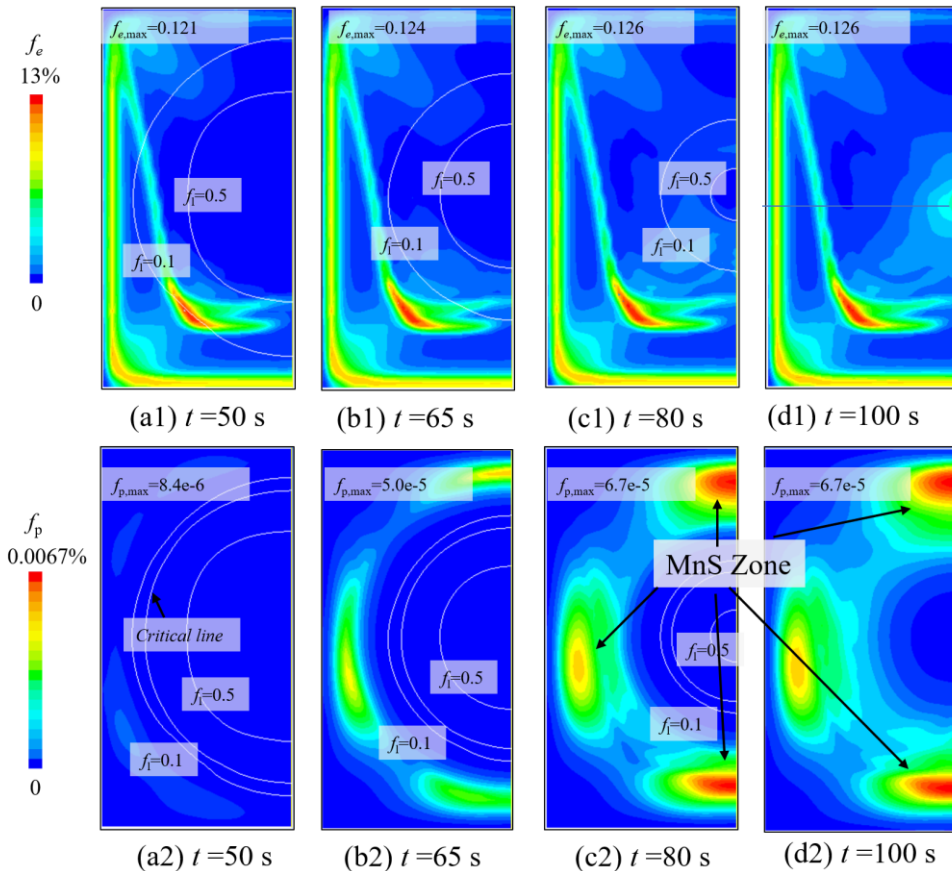


Evolution of Macrosegregation



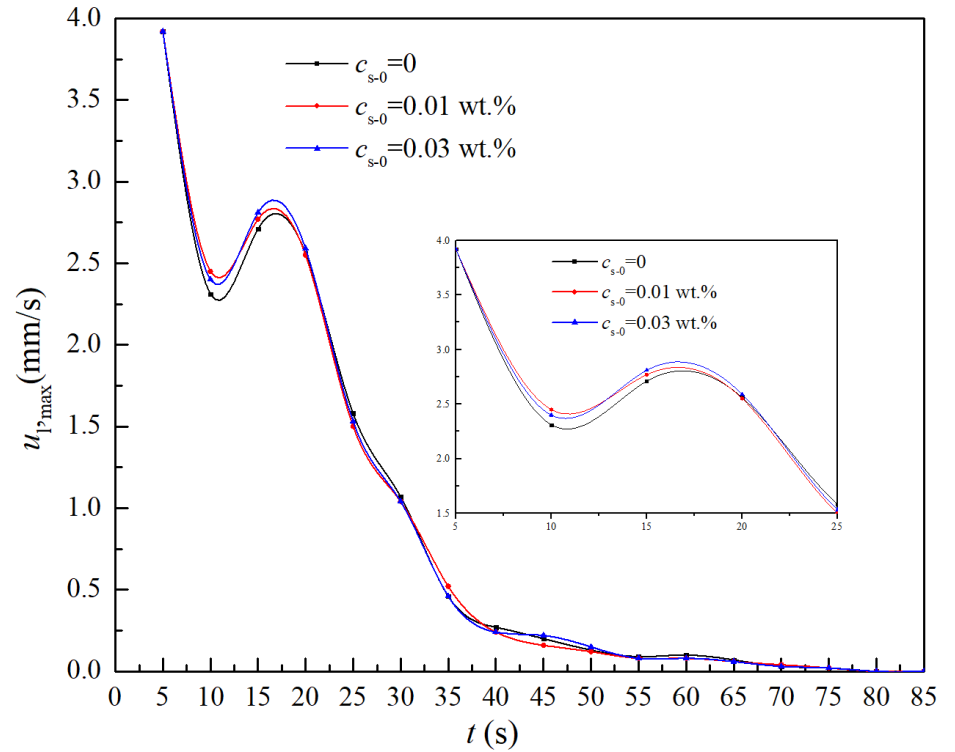
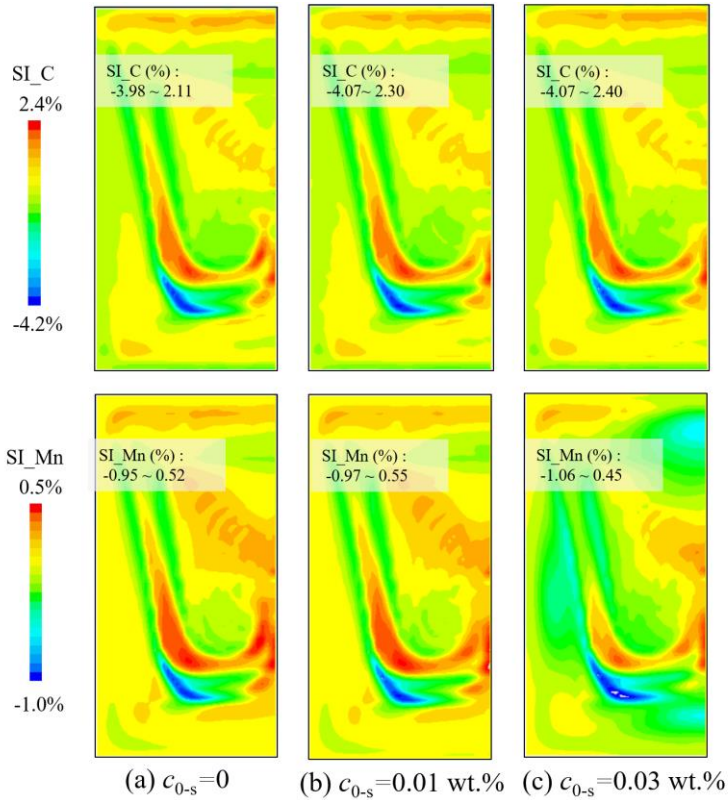
- The sedimentation of equiaxed grains drag the liquid flow downwards
- After 50s, with liquid velocity approaching 0, macrosegregation pattern remains for C, Mn continue to change due to MnS.

■ Distribution of Equiaxed and MnS Phases

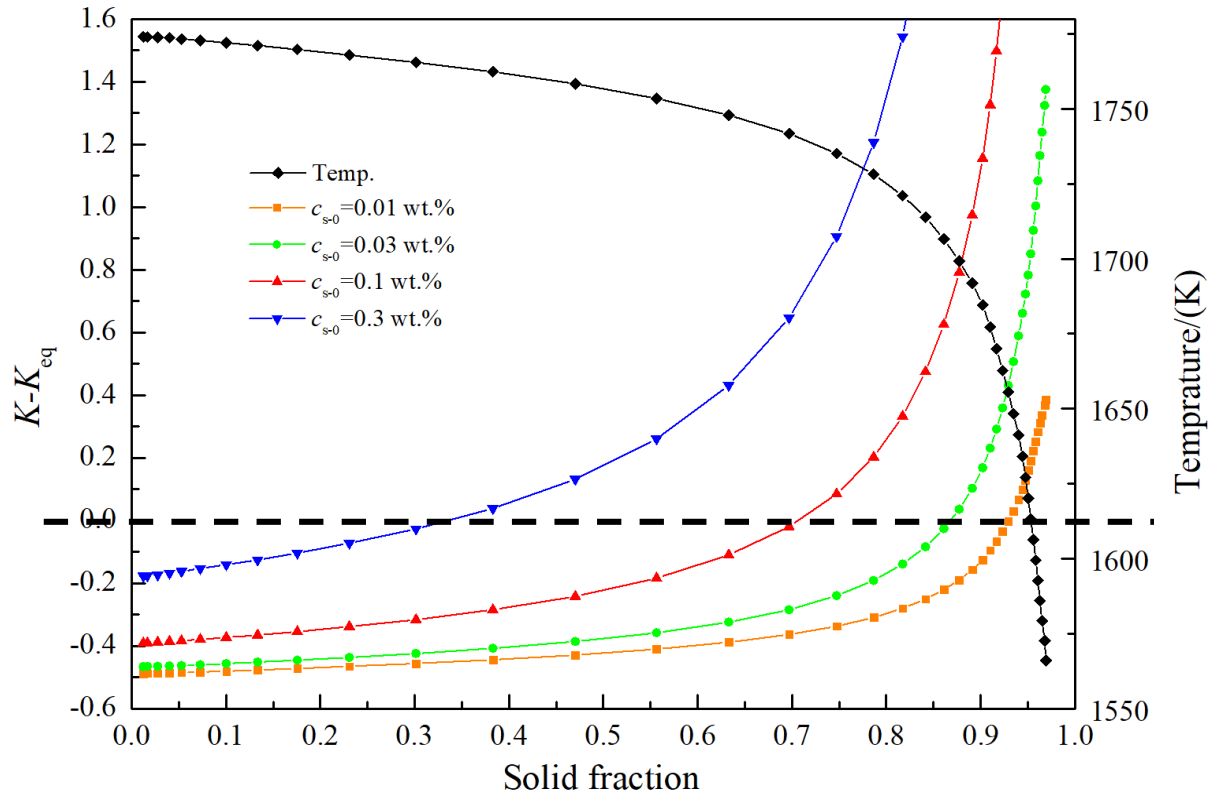


- MnS inclusions mostly locate around a quarter of the whole calculation domain
- Grow velocity of solid at the out layer is too fast to form any inclusions
- The inner zone that solidifies at last has very low Mn solute concentration during overall process.

Effect of S on Macrosegregation



■ Critical Condition of MnS Formation



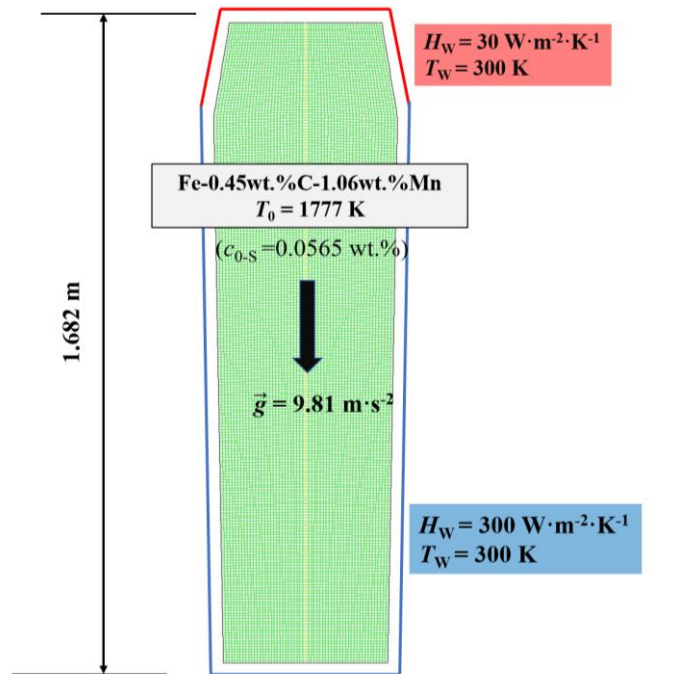
c_{s-0}	f_s	Temperature (K)
0.01wt.%	93.5%	1648.36
0.03wt.%	87.7%	1699.25
0.1wt.%	74.7%	1735.19
0.3wt.%	38.2%	1762.42



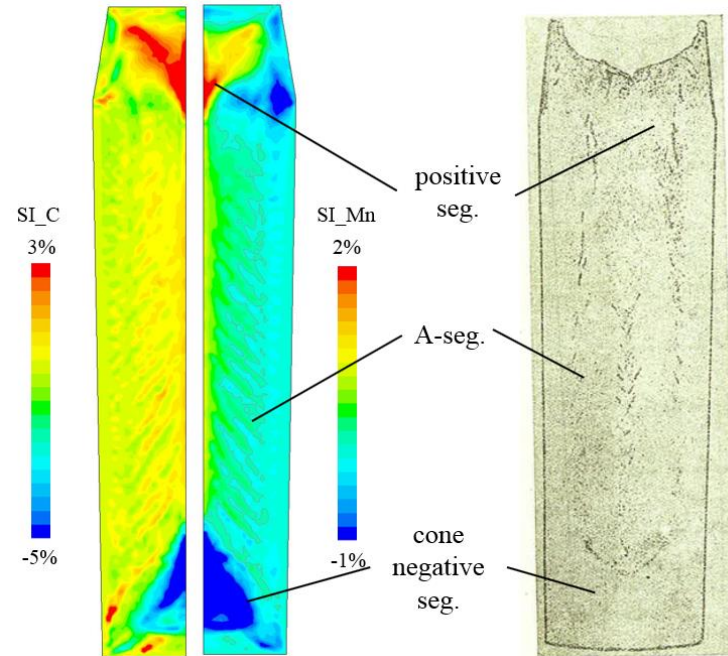
$$K = c_{l,\text{Mn}} \cdot c_{l,\text{S}}$$

$$\log K_{\text{eq}} = -8750/T + 4.63$$

Model Application on Industrial Ingot

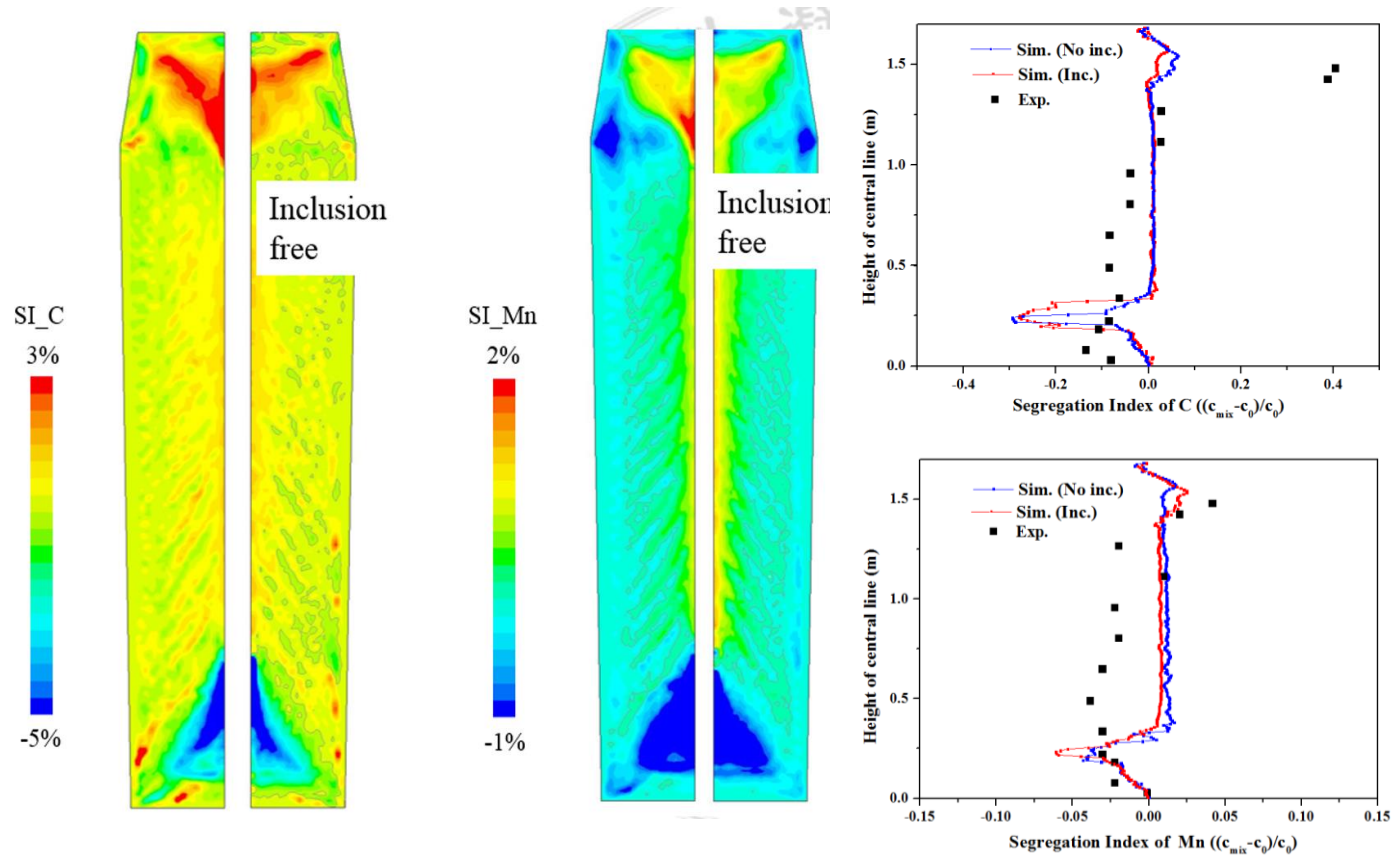


Configuration of 2.45-ton ingot: BC & IC



Comparison of SI of Ternary Model

Model Application on Industrial Ingot



- The bottom negative zone of C is enlarged. The MnS in the mushy zone accelerates the falling amount of equiaxed.
- MnS affects Mn segregation by means of consuming Mn. The overall segregation value in the central line is reduced.

Summary

1

An inclusion-combined macrosegregation model has been established coupling the inclusion growth theory with multicomponent multiphase solidification.

2

The effects of MnS behavior on macrosegregation of C and Mn are different; the former is changed by altering the flow field of phases while the latter is mainly affected by solute consumption.

3

The critical condition of MnS precipitation in Fe-0.45 wt.%-1.06 wt.% steel can be calculated given a certain S composition.

4

By the integrated effects of solidification velocity, columnar growth, and Mn solute diffusion, MnS inclusions mostly locate at half central of whole solidification domain

University of Leicester

THANK YOU

Duanxing Cai, Jun Li, Hongbiao Dong and Jianguo Li---A comprehensive model for the coupled modelling of MnS inclusion and macrosegregation